

See discussions, stats, and author profiles for this publication at: <https://www.researchgate.net/publication/259491482>

Tunable Reverse-Biased Graphene/Silicon Heterojunction Schottky Diode Sensor

Article in *Small* · April 2014

DOI: 10.1002/sml.201302818 · Source: PubMed

CITATIONS

29

READS

213

4 authors:



Amol Singh

University of South Carolina

23 PUBLICATIONS 223 CITATIONS

SEE PROFILE



Md Ahsan Uddin

Clemson University

20 PUBLICATIONS 73 CITATIONS

SEE PROFILE



Tangali Sudarshan

University of South Carolina

352 PUBLICATIONS 2,674 CITATIONS

SEE PROFILE



Goutam Koley

Clemson University

94 PUBLICATIONS 1,586 CITATIONS

SEE PROFILE

All content following this page was uploaded by [Goutam Koley](#) on 09 June 2014.

The user has requested enhancement of the downloaded file. All in-text references [underlined in blue](#) are added to the original document and are linked to publications on ResearchGate, letting you access and read them immediately.

Tunable Reverse-Biased Graphene/Silicon Heterojunction Schottky Diode Sensor

Amol Singh,* Md. Ahsan Uddin, Tangali Sudarshan, and Goutam Koley

A new chemical sensor based on reverse-biased graphene/Si heterojunction diode has been developed that exhibits extremely high bias-dependent molecular detection sensitivity and low operating power. The device takes advantage of graphene's atomically thin nature, which enables molecular adsorption on its surface to directly alter graphene/Si interface barrier height, thus affecting the junction current exponentially when operated in reverse bias and resulting in ultrahigh sensitivity. By operating the device in reverse bias, the work function of graphene, and hence the barrier height at the graphene/Si heterointerface, can be controlled by the bias magnitude, leading to a wide tunability of the molecular detection sensitivity. Such sensitivity control is also possible by carefully selecting the graphene/Si heterojunction Schottky barrier height. Compared to a conventional graphene amperometric sensor fabricated on the same chip, the proposed sensor demonstrated 13 times higher sensitivity for NO_2 and 3 times higher for NH_3 in ambient conditions, while consuming ~ 500 times less power for same magnitude of applied voltage bias. The sensing mechanism based on heterojunction Schottky barrier height change has been confirmed using capacitance-voltage measurements.

1. Introduction

Graphene has drawn a huge research interest in the past several years due to its extraordinary material properties^[1] including remarkably high charge carrier mobility of $200\,000\text{ cm}^2\text{ V}^{-1}\text{ s}^{-1}$ in suspended form,^[2] very high surface to volume ratio due to its essentially two-dimensional (2D) nature,^[3] and very low Johnson noise in the limit of no charge carriers.^[3–5] These properties make graphene very attractive for molecular sensing applications, since the adsorbed molecules can readily affect its conductivity through charge transfer.^[3] Demonstration of its ultra-high sensitivity, down

to a single gas molecule,^[3] has generated widespread interest in its potential application for molecular detection based on changes in conductance,^[3,6,7] surface work function,^[6] frequency of the surface acoustic waves,^[8] as well as low frequency noise spectra.^[7,9]

A vast majority of the graphene based sensors reported so far are in the form of chemiresistor or chemical field effect transistors (Chem-FETs) where the surface adsorbed molecules proportionally change the charge carrier density in graphene causing its conductivity to vary in direct proportion with the number of adsorbed molecules. The detection sensitivity in these sensors, for a specific analyte, is determined by the mobility of the carriers in graphene (since conductivity is proportional to the product of mobility and charge density), and hence largely dependent on the substrate the graphene film is synthesized on or transferred to.^[10] Although the sensitivity of these sensors can be tuned by utilizing a back-gate as demonstrated recently,^[11] it requires additional bias source and complicity in sensor design.

Recent investigations on graphene/semiconductor heterojunction Schottky diodes^[12–14] have opened up the possibility for developing interesting electronic devices, such as

A. K. Singh,^[+] M. A. Uddin,^[+] Prof. T. S. Sudarshan, Dr. G. Koley
Department of Electrical Engineering
University of South Carolina
Columbia, SC, 29208, USA
E-mail: singhak@email.sc.edu



^[+]These authors contributed equally to this work.

DOI: 10.1002/sml.201302818

insulated top gate transistor called “Barristor”.[15] Such heterojunctions are not only fundamentally attractive from the perspective of electronic devices, but also very promising for sensing applications due to the atomically thin nature of graphene, which allows modulation of the graphene Fermi level, and consequently the interface Schottky barrier height (SBH) of the graphene/semiconductor junction, by molecules adsorbed on the outer surface of graphene. Thus, the reverse current flowing across the junction can vary exponentially with change in SBH which is proportional to the density of adsorbed molecules. Sensing response of the heterojunction diode has been demonstrated very recently with the diode operating in forward bias.[16] However, in forward bias, the series resistance of the diode dominates after turn-on voltage, and change in overall sensor resistance due to adsorbed molecules is dominated by the change in diode series resistance (mainly graphene), thus the exponential change in current with change in SBH is generally not observed. On the other hand, when operated in reverse bias, the current (thermionic emission) can change exponentially with change in SBH, unlike in forward bias operation (dominated by series resistance), or in chemiresistor type sensors, where a linear response is expected with molecular adsorption. The reverse bias operation also offers the advantage of tuning the sensor sensitivity through bias dependent modulation of the graphene Fermi level and hence the SBH. In addition, the reverse bias operation results in a drastic reduction in the operating power requirement of the sensor (with consequent minimization of heating effects) which is highly desirable from the sensor design perspective. In this work, we have demonstrated for the first time, dramatically improved sensing response of reverse biased graphene/Si heterojunction

Schottky diodes compared to regular chemiresistor type sensors. It was further observed that the sensor sensitivity can be tuned through variation in the diode reverse bias magnitude and careful selection of the heterostructure Schottky diode barrier height.

2. Results and Discussion

Top panel of **Figure 1a** shows a typical Raman spectrum for the as-grown CVD graphene on copper foil showing signature D, G, and 2D peaks. The I_D/I_G ratio of 0.2 indicates good quality of the graphene.[17] The I_G/I_{2D} ratio of 3.9 and 2D peak full width at half maximum (FWHM) of $\sim 21.33 \text{ cm}^{-1}$ indicates the presence of single layer graphene.[18] Raman spectra of graphene transferred on Si and SiO_2/Si substrates from one of the graphene/p-Si devices are also shown in the middle and bottom panels of **Figure 1a**. Schematic diagram of the graphene/Si heterojunction diode sensor, along with graphene chemiresistor sensor fabricated by its side for direct performance comparison, is shown in **Figure 1b**. **Figure 1c** shows the optical image of a fabricated graphene/p-Si sensor device. Electrical characterization of the graphene/Si heterojunction showed Schottky type current-voltage (I - V) characteristics, which is in agreement with earlier reports (voltage bias was applied to the Si contact for both p- and n-Si diodes and the graphene contact was grounded).[12] Representative I - V characteristics for graphene/p-Si and graphene/n-Si heterojunction Schottky diodes are shown in **Figure 2**. In both cases, the diode current increases exponentially with voltage initially (up to $\sim 1\text{V}$, see inset plots), before being dominated by series resistance. Nonetheless, these results are

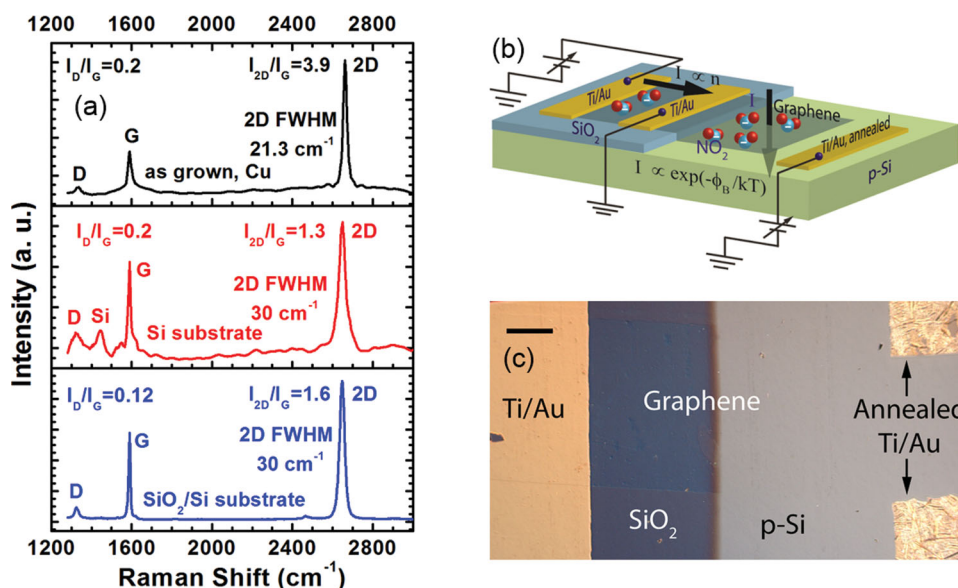


Figure 1. (a) Representative Raman spectra of CVD graphene grown on copper (top panel), transferred on Si (middle panel) and SiO_2/Si (bottom panel) substrate showing the characteristic G, D and 2D peaks. (b) Device schematic and biasing scheme of graphene chemiresistor and graphene/Si Schottky diode sensor fabricated on the same chip. Chemiresistor is a case of lateral transport where current is proportional to number of charge carriers in graphene. Whereas the carrier transport across the vertically stacked graphene/p-Si heterojunction results in current that is exponentially dependent upon SBH under reverse bias condition. (c) Optical micrograph of a graphene/p-Si Schottky diode illustrating transferred graphene on SiO_2 and p-Si, Ti/Au contact on graphene and annealed Ti/Au contact on p-Si. The scale bar is 200 μm .

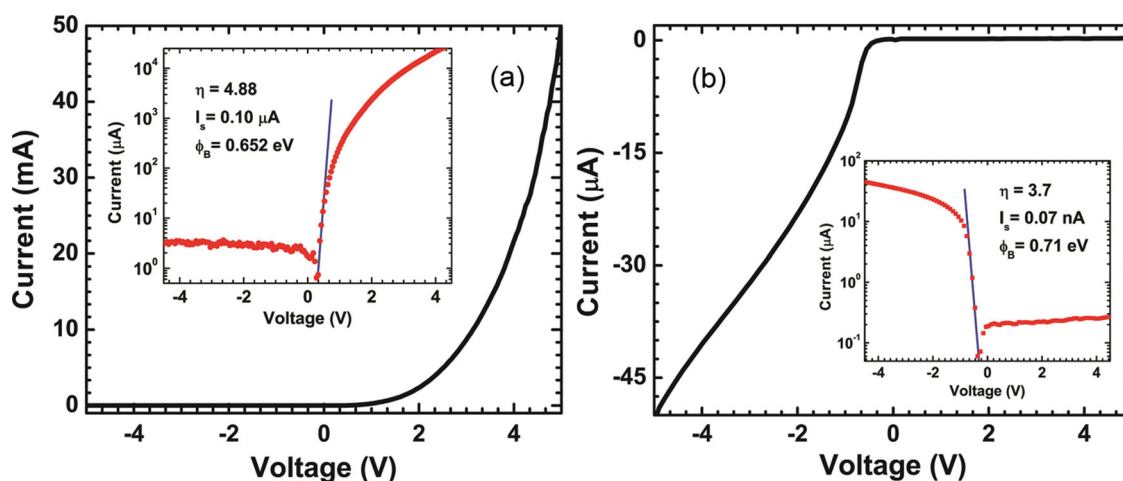


Figure 2. Current-Voltage (I - V) characteristics of (a) graphene/p-Si and (b) graphene/n-Si devices showing rectifying behavior. Here n-/p-Si is connected to the positive and graphene is connected to the negative terminal of a Source Measure Unit. I - V characteristics in logarithmic scale shown in the inset exhibit 4 and 3 orders of magnitude change in current for graphene/p-Si and graphene/n-Si devices, respectively.

consistent with recent reports,^[12] indicating that graphene forms Schottky contact with both n-type and p-type Si. This is expected since the reported work function for graphene of 4.5 eV is about midway between the work functions for p-type and n-type Si with electron affinity of 4.05 eV and

bandgap of 1.12 eV at room temperature.^[19] Examining the insets in Figure 2, we find that in reverse bias the current increases monotonically with increasing bias magnitude (more clearly seen in **Figure 3** for ambient I - V measurements in solid black line). This is because with increase in reverse

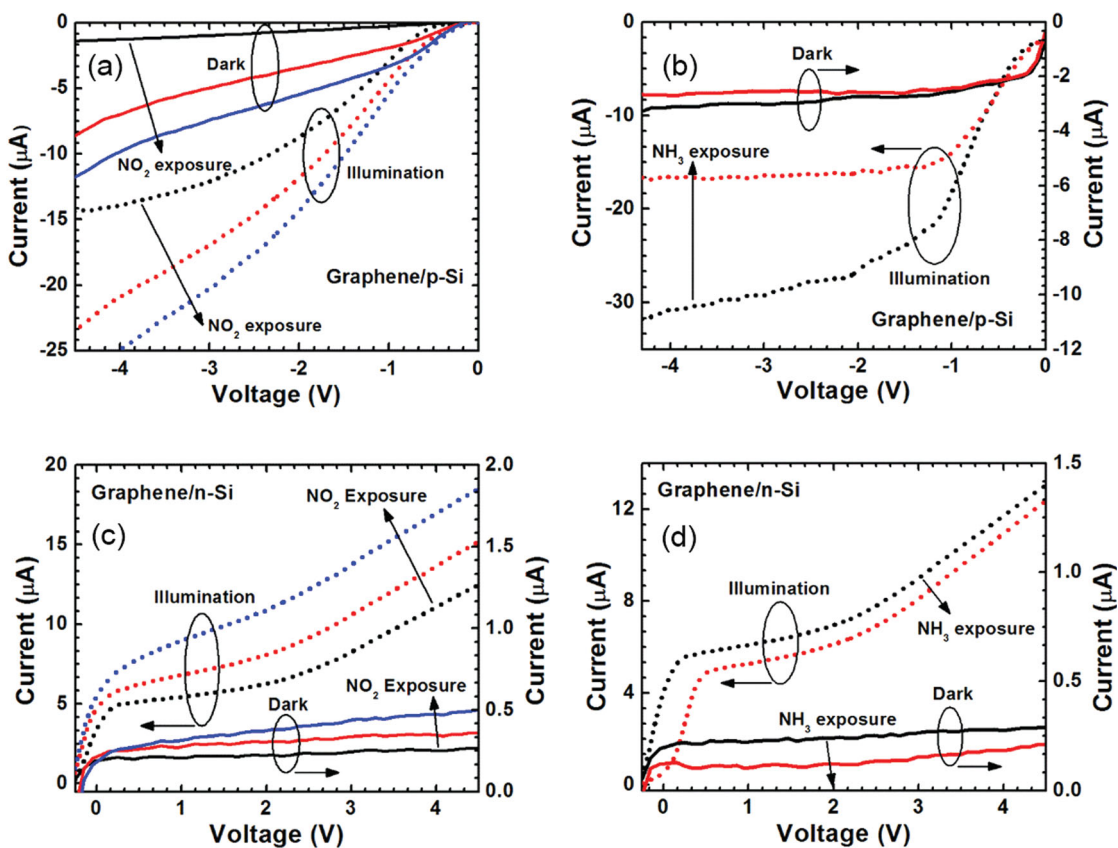


Figure 3. Reverse bias current-voltage characteristics of graphene/p-Si Schottky diode in dark and in illumination for different exposure times of (a) NO_2 and (b) NH_3 . The solid curves correspond to measurements in dark condition and dotted curves to those under illumination. The black (both solid and dotted) curves represent pre-exposure characteristics, while the red and blue curves represent those after 10 min and 30 min of gas exposure. Reverse current across the graphene/n-Si heterojunction device (c) is increasing for NO_2 and (d) decreasing for NH_3 . Complete I - V characteristics for all the four cases are given in supporting information, Figure S1.

bias graphene's work function changes (due to change in carrier concentration), which causes a lowering of the SBH.^[20,21] The ideality factor and SBH can be extracted from the diode characteristics of Graphene/p-Si and n-Si devices which can be expressed by the thermionic emission model given by Equation (1).^[19]

$$I = I_s \left[\exp\left(\frac{qV}{\eta kT}\right) - 1 \right] = AA^*T^2 \exp\left(-\frac{\phi_B}{kT}\right) \left[\exp\left(\frac{qV}{\eta kT}\right) - 1 \right] \quad (1)$$

Here, I_s is the reverse saturation current, q is the electronic charge, A is the contact area, A^* is the effective Richardson Constant, η is the diode ideality factor, T is the temperature, ϕ_B is the SBH, and k is the Boltzmann constant. When plotted in logarithmic scale, Equation (1) would be linear for $V \gg \eta kT$ until much higher bias voltage ($\sim 1V$) where series resistance starts to dominate. From the slope of this linear segment of the I-V plot, one can determine η , while the intercept on y-axis will give the saturation current, from which the SBH can be determined with the knowledge of the diode area A and Richardson's constant A^* . The insets of Figure 2a,b show the logarithmic I-V plots for graphene Schottky junctions with p- and n-Si, respectively. Using these plots, and the measured area of $9 \times 10^{-3} \text{ cm}^2$ and A^* values of 46.32 and $252 \text{ Acm}^{-2}\text{K}^{-2}$ for p-Si^[22] and n-Si,^[13] respectively, we find $\eta = 4.88$, and $\phi_B = 0.65 \text{ eV}$ for the former, and $\eta = 3.7$ and $\phi_B = 0.71 \text{ eV}$, for the later. These values are in close agreement with those reported recently.^[13,21] Notably, for these junctions, $\eta > 1$ is commonly observed, which has been attributed to barrier height variation with reverse bias arising from graphene's bias dependent work function, image charge induced Schottky barrier lowering, and Schottky barrier inhomogeneity.^[20,21,23]

To investigate the influence of molecular adsorption (chemical doping) on charge transport across the graphene/Si heterojunction (which determines the sensitivity of the sensor), the I-V characteristics upon exposure to dilute NH_3 and NO_2 gases (typically electron donating and accepting, respectively) were recorded for both Graphene/p-Si and n-Si heterojunctions. We define the sensor response as $(I - I_0)/I_0$ expressed in percentage, where I_0 is the initial sensor current, and I is the current after exposure to an analyte gas. Initially, we used 20 ppm NO_2 and 550 ppm NH_3 to study the responses in both dark and illuminated (using light from a halogen lamp using a fiber optic cable) ambient conditions. The reverse bias I-V characteristics of the graphene/p-Si diode sensor recorded after different durations of exposure to NO_2 and NH_3 are shown in Figure 3a,b respectively (entire I-V characteristics of the diodes with NO_2 and NH_3 exposure is included in the supporting information, Figure S1). We find that with NO_2 exposure, the current increases dramatically both in dark and illuminated conditions due to lowering of the SBH. For example, at $-4V$ bias, the current increased more than 8 times from 1.2 to $9.8 \mu\text{A}$ (a change of 716%) with 30 min of NO_2 exposure in dark, while it increased from 13.9 to $24.9 \mu\text{A}$ (a change of 79%) for the same duration under illumination. In contrast, for NH_3 exposure the change (reduction) in current is rather small in dark (13.6%), but improves under illumination (Figure 3b), with the current

decreasing from 30.5 to $17.4 \mu\text{A}$ after 30 min exposure (a change of 43%). The response for NO_2 is extremely large, and to the best of our knowledge have not been observed with any graphene based sensor in ambient conditions till date, where typical conductivity changes range from a few percent to a few tens of percent.^[24-28] Clearly, this sensing modality opens up a new paradigm for developing sensors with ultra-high sensitivity. Since adsorption of NH_3 is expected to increase the SBH,^[6,29] when the current is already small, i.e. the SBH is high, the change in current is not very large. However, under illuminated conditions, when the current has increased significantly due to excess carrier generation and barrier lowering, the reduction in current is much more noticeable. The above factor also contributes to the observation of much lower sensing response (percentage change in current) for NH_3 (43%) compared to NO_2 (716%), where the later, in addition to lowering the SBH due to adsorption, also participates in a much larger charge exchange with graphene^[30] to produce a much larger sensing response. An interesting point to note from Figure 3 is that the response for NO_2 is much faster than NH_3 , and it does not saturate with time, i.e. the current change for 30 min exposure is much larger than that for 10 min exposure, unlike NH_3 where the current saturates rather quickly which is experimentally observed for different conditions and is discussed in detail later. For, Graphene/n-Si devices, similar responses have been obtained, i.e. NO_2 response (Figure 3c) is large and increases with exposure time, while for NH_3 (Figure 3d), there is clear distinctive response in presence of both dark and light, but it saturates quickly.

To determine the magnitude of change in SBH at graphene/Si heterojunction due to molecular adsorption, capacitance-voltage (C-V) measurements were performed (details are included in the supporting information, Figure S2). The $1/C^2$ vs. V_R plots obtained for 20 min of NO_2 and NH_3 exposure are compared to those obtained prior to gas exposure in Figure 4a. The built-in voltage, V_{bi} can be determined from the relationship between the C^{-2} and applied reverse bias V_R given as:

$$C^{-2} = 2(V_{bi} + V_R)/(q\epsilon_s N_{A/D}) \quad (2)$$

Here q is the electronic charge, ϵ_s is the semiconductor permittivity, and $N_{A/D}$ is the acceptor/donor doping.^[31] From extrapolating the plots, the built-in voltages (V_{bi}) are determined as 0.69 eV for pre-exposed condition, and 0.46 and 0.85 eV after 20 min exposure to NO_2 and NH_3 , respectively. The graphene/p-Si SBH is given as, $\phi_B = V_{bi} + (E_F - E_V)$, where E_F is the Fermi level and E_V is the valance band edge of Si. $E_F - E_V$ is estimated to be -0.2 eV for the p-type Si used from the resistivity of $1 - 10 \Omega\text{cm}$ specified by the manufacturer. Thus, the pre-exposed SBH becomes 0.89 eV , which is in good agreement with earlier results.^[14,21] Figure 4b illustrates the time evolution of V_{bi} from initial steady state value in ambient condition, as the 20 ppm NO_2 flow is started over the sensor and stopped, and 550 ppm NH_3 flow is started and stopped, successively. As expected, we find that V_{bi} keeps on decreasing from the initial steady state value of 0.69 eV

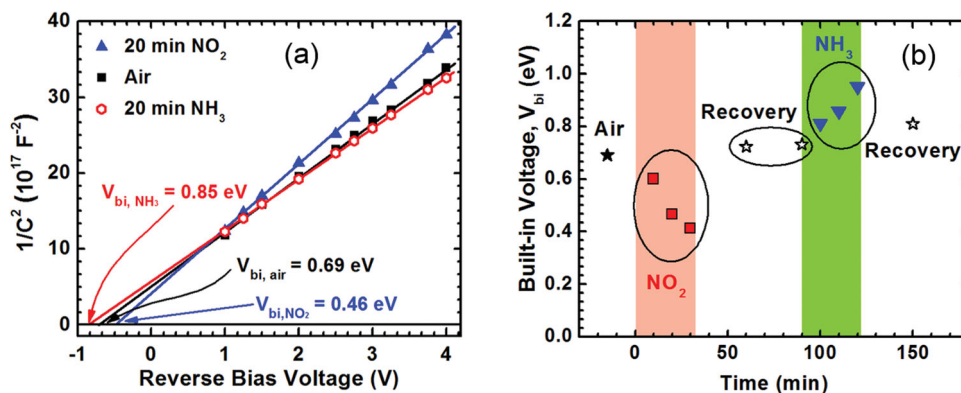


Figure 4. (a) Built-in voltage extracted from the C^{-2} vs. reverse voltage plot for graphene/p-Si in ambient condition (black square), in NO_2 (red hexagon) and in NH_3 (blue triangle). The gas exposure duration was 20 min for both NO_2 and NH_3 . (b) Time evolution of extracted built-in voltage in the different conditions: in ambient air, NO_2 exposure, at recovery, NH_3 exposure and at recovery again.

upon exposure to NO_2 , and then recovers back close to the initial value as the NO_2 flow is stopped. It further continues to rise with NH_3 exposure, and recovers back to the original steady state value as the NH_3 flow is stopped. We find that the change in V_{bi} , and hence in SBH, due to NO_2 exposure is larger than that due to NH_3 exposure (0.23 and 0.16 eV, respectively, in 20 min), in spite of the much higher concentration of the later. This can be attributed to the weak electron donating nature of NH_3 (0.03q) compared to the strong electron accepting (0.3q) nature of NO_2 .^[30] The SBH determined from C-V measurements is higher than that obtained from I-V measurements, i.e. 0.89 and 0.65 eV, respectively for graphene/p-Si diodes (steady state value in ambient). The difference can arise partly from the uncertainty in determining $E_{\text{F}} - E_{\text{V}}$ (see above discussion), and also from Schottky barrier inhomogeneity and additional leakage paths at the junction, which generally underestimates the SBH determined from I-V measurements.^[20,21,23]

Compared to the sensing responses observed in reverse bias, the forward bias responses for both NO_2 (20 ppm) and NH_3 (550 ppm) are significantly lower, i.e., 92% and 6.5% at 4V bias for graphene/p-Si Schottky diode, compared to 716% and 43% for 4 V reverse bias, respectively (change in the entire I-V characteristics of the diodes with NO_2 and NH_3 exposure is included in the supporting information, Figure S1). This can be attributed to the effect of diode series resistance which becomes significant for forward bias operation, as discussed earlier. Similarly, our responses of 43% obtained at -4V bias for 550 ppm NH_3 is much improved compared to the forward bias response of only a few percent obtained for graphene/Si Schottky diode sensor for 4% NH_3 as reported in reference.^[15] Although, biasing the diode in the sub-threshold region can minimize the effect of diode series resistance, it is difficult to reliably bias a sensor in this region due to environmental factors affecting the turn-on voltage. In addition, it would not be possible to tune the diode sensitivity in forward bias as it can be done in reverse bias.

To make a direct comparison of the performance of the graphene/Si heterojunction diode sensor and conventional graphene chemiresistor type sensor, both the devices were

fabricated side by side on the same chip from the same transferred graphene film. The chemiresistor was fabricated on SiO_2 covered area of a Si substrate, while the heterojunction diode sensor was fabricated on bare Si with SiO_2 etched away, as shown schematically in Figure 1b. The I-V characteristics of graphene Chemiresistor is included in supporting information, Figure S3. The responses from the two sensors are compared in Figure 5a for 10 min NO_2 exposure (shaded region). We observe that the chemiresistor current changes by only 7.8 %, increasing from 1.027 to 1.1065 mA, while that in the diode sensor changes by 104 % increasing from 2.12 to 4.34 μA , under the same applied bias magnitude of 4 V (reverse bias for the diode sensor). This constitutes a 13.3 times enhancement in response for the diode sensor compared to the regular chemiresistor sensor, clearly highlighting the improved performance of the former. For NH_3 the difference in response is less dramatic, but a significant 3 times higher response is observed for Graphene/p-Si diode sensors compared to the graphene chemiresistor (Figure 5b). Very significantly, the reverse bias operation of the diode sensor enables it to operate at a much lower power level of 2.12 $\mu\text{A} \times 4 \text{ V} = 8.48 \mu\text{W}$ compared to the chemiresistor, which requires an operational power of 1.027 mA $\times 4 \text{ V} = 4.108 \text{ mW}$, a reduction of 484 times, which is highly desirable for sensor system design.

Careful observation of Figure 5a,b indicates that exposure to NO_2 results in a fast and almost linearly changing conductivity, which does not saturate even after 10 min of exposure. In contrast, with NH_3 exposure, the conductivity changes at a slower rate (in terms of percentage change), and reaches a constant value in 1–2 min. This can be explained by considering previously reported results that the propensity for charge transfer between adsorbed molecules and graphene decreases as the graphene Fermi level moves closer to the defect level introduced by the adsorbed molecules.^[11] Initially, the graphene Fermi level, though below Dirac point, is much closer to the NH_3 induced defect level, which is slightly above the Dirac point, compared to NO_2 defect level which is typically formed 300–400 meV below the Dirac point (Figure 5c shows the band diagram for graphene/p-Si heterojunction along with the NO_2 and NH_3 induced defect

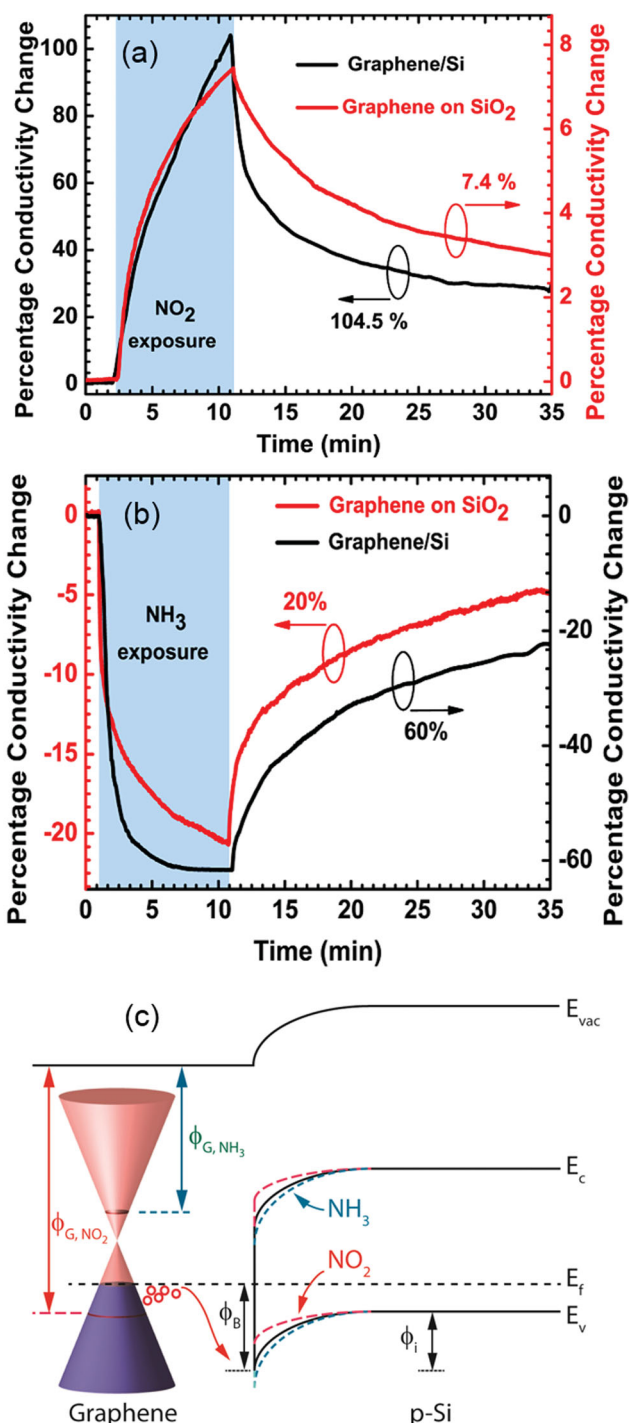


Figure 5. (a) Comparison between the NO₂ responses of graphene/p-Si heterojunction device and graphene chemiresistor on SiO₂ fabricated on the same chip side by side. The black line shows the response of graphene/p-Si device and red line shows the response of graphene on SiO₂ for NO₂ exposure. The exposure duration (10 min) and bias voltage magnitude (4 V) is same for both the cases where reverse bias is applied across the graphene/p-Si device. (b) Comparison of NH₃ sensing behavior where the black and red lines show the responses of the graphene/p-Si device and graphene chemiresistor, respectively, for NH₃ exposure. (c) The energy band diagram of Graphene/p-Si heterostructure in three different conditions, showing reduction in SBH for NO₂, and increase in SBH for NH₃ exposure, as compared to the pre-exposure condition.

levels).^[11,30,32] Therefore, the charge transfer process between NO₂ and graphene is much faster compared to NH₃, for which the response saturates as the Fermi level reaches close to the defect energy level introduced by its adsorption. To verify this idea further, we performed a series of measurements and studied the response as a function of concentration, exposure time and reverse bias voltage.

Figure 6a shows the sensor response as a function of NO₂ concentration downward from 20 ppm. We find that a concentration down to 200 ppb can be sensed easily, although the response is slower for lower concentrations, probably due to the sensor operation in ambient conditions. The response plotted as a function of concentration in logarithmic scale (Figure 6b) shows a linearly increasing sensitivity from 7 to 410% for a concentration variation from 200 ppb to 20 ppm. The NH₃ response for 5 min exposure is shown in Figure 6c with concentrations varying from 10 to 550 ppm. The response magnitude can be seen to increase logarithmically with the increase in concentration as shown in Figure 6d. However, a logarithmic plot of percentage resistivity change as a function of concentration is almost linear as seen in Figure 6d. For 10 ppm, the conductivity magnitude change is 43.4% which increased to 93.3% for 550 ppm NH₃. The corresponding resistivity change is 76.6% for 10 ppm and an enormous 1392.5% for 550 ppm NH₃. To investigate the repeatability of the reverse biased sensor response, it was exposed to 20 ppm NO₂ and 50 ppm NH₃ for 4 successive cycles, and the responses are shown in Figure 6e and f, respectively. For the initial NO₂ exposure, the graphene/p-Si sensor shows 64% increase in conductivity in 10 minutes. The recovery was carried out in ambient condition for the same time duration (10 minutes), and the sensor recovered to less than 20% of the maximum response (Figure 6e). For the subsequent cycles the sensor showed very good repeatability, although the maximum value of the response increased slightly in every cycle due to incomplete recovery. The graphene/p-Si sensor showed very repeatable responses for 50 ppm NH₃ as well, when exposed to 5 min on/off duration for 4 consecutive cycles. For the initial NH₃ exposure, the sensor showed 66% decrease in the conductivity and in 5 min recovered to less than 20% in ambient condition (Figure 6f). Very similar responses were recorded for the next 3 cycles. Thus, we find that for both electron acceptor and donor type of gas molecules the diode sensor responses are quite repeatable. Although we have included sensing response down to 200 ppb of NO₂, with proper optimization of the sensor, detection down to low ppb range is anticipated. In the low frequency range (≤ 100 KHz), which is relevant for sensor operation, the ultimate sensor performance is typically limited by the 1/f noise, which in graphene chemiresistor sensors arises out of the fluctuations in number of charge carriers and mobility caused by charged impurities and scattering centers.^[33] For the proposed sensor based on graphene/Si heterojunction, the 1/f noise is still expected to be predominant in low frequencies, however, the factors affecting it need to be carefully investigated, especially bearing in mind that the overall noise is affected by current transport through a graphene resistor, a graphene/Si heterojunction and a Si resistor.

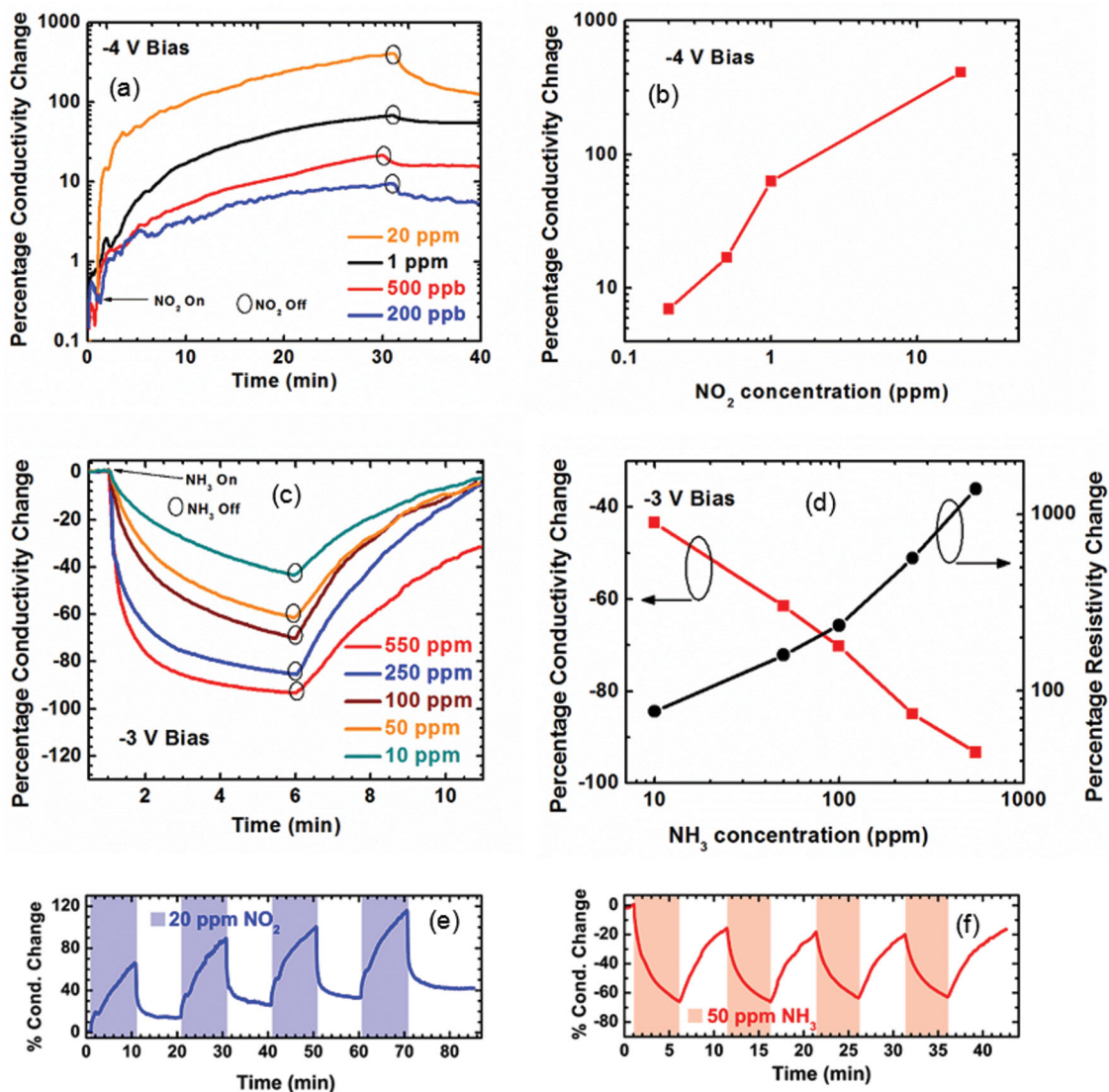


Figure 6. (a) Sensor response for different NO₂ concentration decreasing from 20 ppm to 200 ppb for 30 min of exposure at -4 V reverse bias. (b) Log-log plot of the maximum conductivity change as a function of NO₂ concentration. (c) Sensitivity plots for different concentration of NH₃ varying from 550 ppm to 10 ppm for 5 min of exposure at reverse bias of -3V. (d) Logarithmic plot of maximum conductivity change along with the corresponding resistivity change with NH₃ concentration. The repeatability of sensor response of the diodes is illustrated for (e) 20 ppm NO₂ and (f) 50 ppm NH₃ sensing.

Figure 7a,b shows the effect of exposure time and bias voltage for NO₂, while those for NH₃ are shown in **Figure 7c,d**. From **Figure 7a,b** we find that simply increasing the duration of exposure to NO₂ does not affect the rate of change of current to a noticeable extent, however, changing the magnitude of the applied reverse bias affects it significantly. With higher reverse bias, the current increases at a faster rate initially, but shows some tapering afterwards, which can be clearly seen for $V_g = -8$ V. With more negative bias applied to p-Si, the graphene Fermi level goes down further away from the Dirac point toward the NO₂ defect level, reducing the SBH. The reduction in SBH causes the junction current to increase, and responses to be faster initially, which however tapers off as the Fermi level approaches the NO₂ defect level (**Figure 7b**). Such tapering effects are clearly seen for NH₃ responses in **Figure 7c,d**, where the responses saturate early, as expected

from discussions above, and do not change with varying exposure time. With the application of higher reverse bias, the Fermi level moves downward, increasing its separation with the NH₃ induced defect level, and causing the NH₃ responses to exhibit less saturating trend as seen from **Figure 7d**.

Although the response and recovery times for the sensors cannot be determined directly from **Figure 7** (since the sensor response did not saturate or recover fully within the time period of measurement), the temporal response of the sensor can still be quantified by the rise rate (percentage change in conductivity per sec), which is typically dependent on the analyte concentration. For NO₂, the extracted rise rate shows a linear increase with the bias voltage, changing from 0.19 to 0.71 percent/sec with increase in reverse bias from -1 to -8 V. This is shown in the supporting information in **Figure S4a**. Rise rate for NH₃ exposure also shows a similar increasing

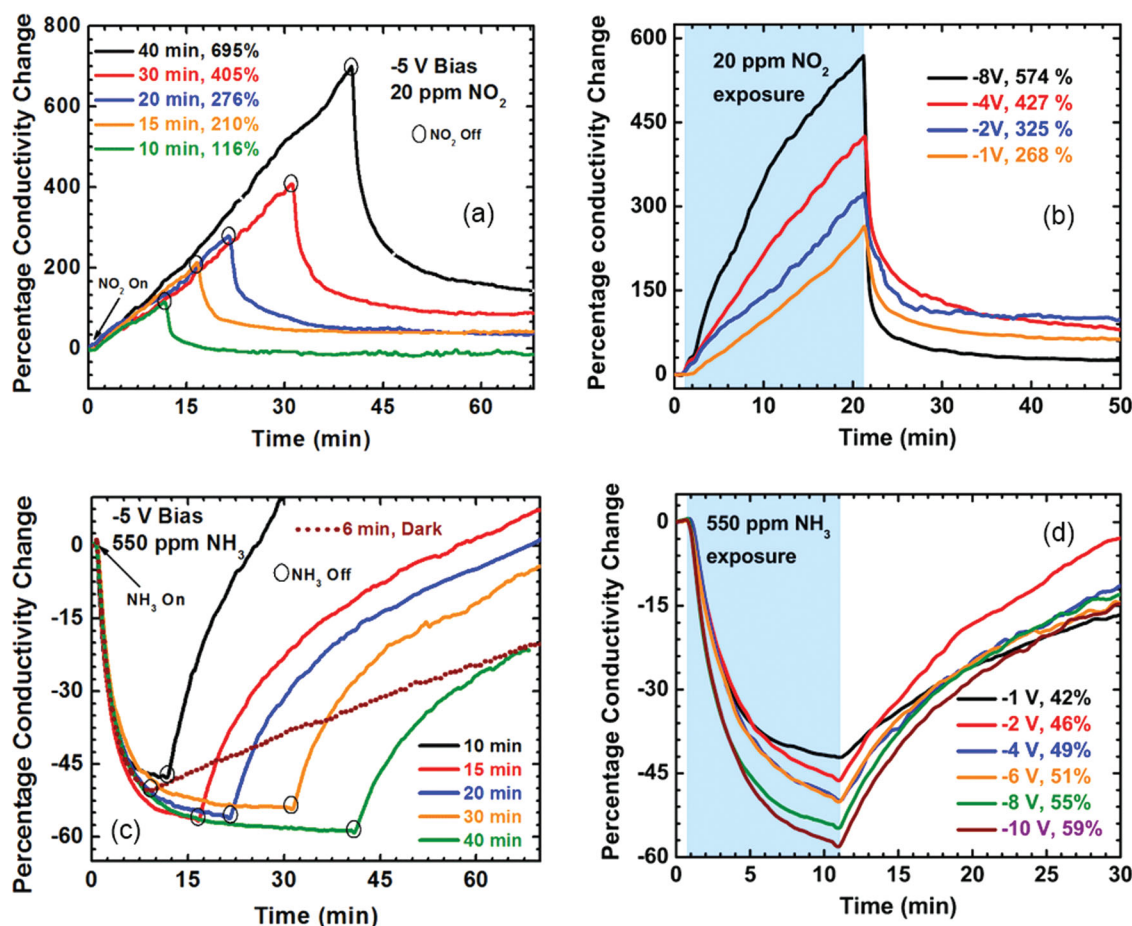


Figure 7. The diode response as a function of exposure time and reverse bias has been illustrated here. (a) Sensitivity to 20 ppm NO₂ for different exposure time where no saturation of the diode is observed till 40 min of exposure. (b) Diode response for 20 min of exposure to 20 ppm NO₂ at varying reverse bias of -1 to -8 V suggesting a tunability of response is possible by varying the reverse bias. (c) Response to 550 ppm of NH₃ with different exposure time. A saturation behavior is observed for current lowering NH₃. (d) Diode response to 10 min of exposure to 550 ppm NH₃ at different reverse bias from -1 to -10 V suggesting a tunable response to NH₃ as well.

trend with the magnitude of the reverse bias (Figure S4b). From Figure 7c we note that the responses measured under illumination have much faster recovery transients compared to the one measured in dark condition. This is because higher photo-generated minority carrier density near the junction under illumination allows the adsorbed NH₃ molecules (positively charged) to become quickly charge neutral and desorb. Careful observation of the recovery transients in Figure 7b indicates that the desorption transient for NO₂ becomes faster with the application of higher negative bias (please refer to supporting information, Table S1). The recovery rate increases from 1.61 to 7.43 percent/sec for the bias voltage increase from -1 to -8 V. For NH₃, the recovery rate increases only slightly from 0.04 to 0.08 percent/sec. Recovery rates for both NO₂ and NH₃ as a function of reverse bias magnitude are plotted in supporting information Figure S4.

It follows from our experimental results that a reverse biased graphene (or another suitable 2D material)/semiconductor “Schottky type” heterojunction can be utilized as a unique platform for developing highly sensitive, fast responding and tunable sensor with a very low operational power requirement. A 2D material, such as graphene, uniquely allows the modulation of the interface SBH while

analyte molecules adsorb on the outer surface. Such a SBH modulation then causes an exponential change in junction current, which imparts them extremely high sensitivity. The low power requirement of the sensor is a direct consequence of its reverse bias operation. Therefore, for optimized sensor design, the Fermi level difference between graphene and the semiconductor needs to be carefully chosen keeping in mind the specific analyte to be detected. For example, with electron acceptor NO₂ and graphene/p-Si diode sensor combination, high sensitivity in conjunction with low operational power can be achieved if SBH is higher and the adsorbing molecules reduce the heterojunction SBH, so that the junction current changes from its usual low value to a higher value. On the other hand, for electron donor NH₃, a lower SBH is preferred so that NH₃ adsorption can increase the SBH and reduce the original higher reverse current to a significant extent which would result in very high sensor response. Our experimental results support these assertions, as illustrated in Figure 8a, where the diode with larger SBH (~ 0.65 eV) shows a much improved response of 104 % for 10 min exposure to 20 ppm NO₂ compared to one with low SBH (~ 0.60 eV), which shows a relatively lower response of 65%. On the other hand, as seen in Figure 8b for NH₃, the sensor diode

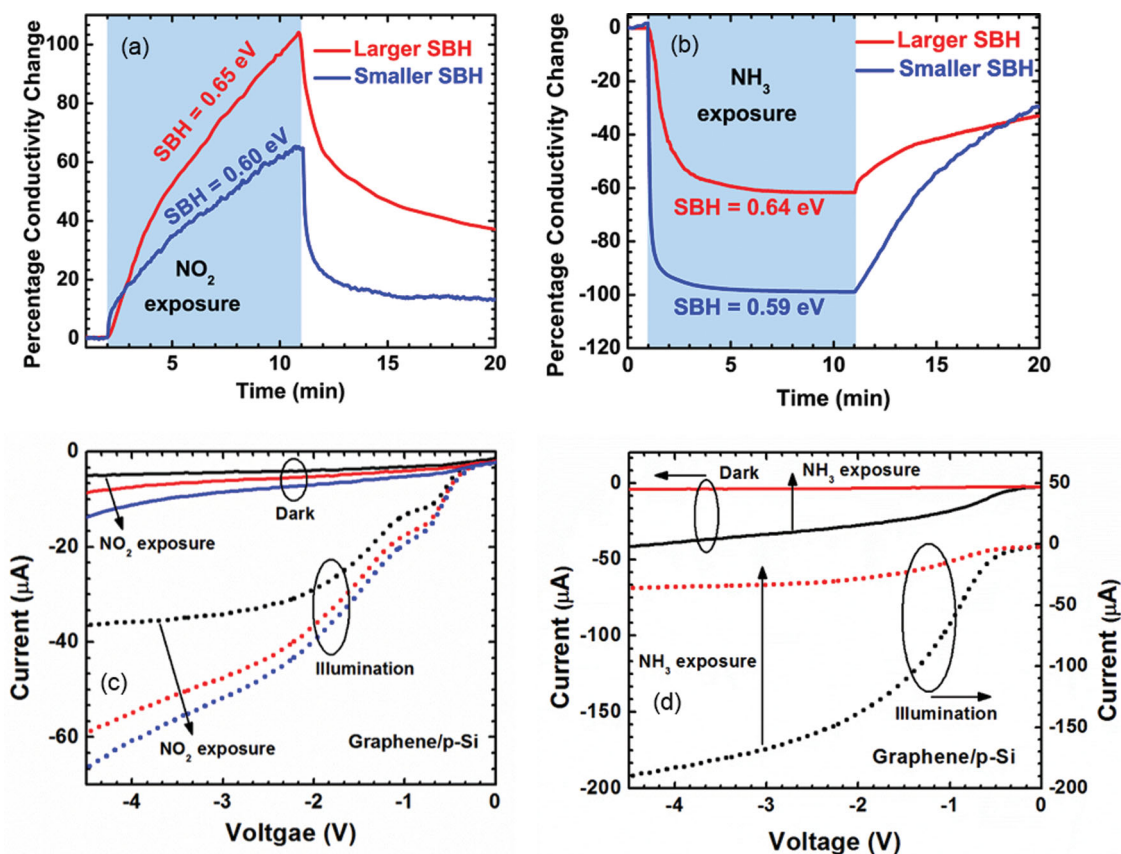


Figure 8. Effect of SBH on Graphene/p-Si heterostructure Schottky diode sensitivity for (a) NO₂ and (b) NH₃. Effects of (c) NO₂ and (d) NH₃ exposure on reverse biased I–V characteristics for a diode sensor. Black curves correspond to pre-exposed condition, solid for dark and dotted for illumination, red curve corresponds to 10 min and blue to 30 min of gas exposure. Lower SBH of the diode sensor results in inferior response to NO₂ exposure (c) and improved response for NH₃ (d) is observed compared to the responses in Figure 3a,b respectively.

with smaller SBH (~0.59 eV) has a much larger response of 99% (resistivity change of 9900%) when exposed to 550 ppm NH₃ for 10 min while a diode with SBH of ~0.65 eV in blue shows a response of 61% (resistivity change of 156%) only. These results are further corroborated through reverse biased I–V characteristics of diode (Figure 8c,d) taken under various gas exposures. A diode with a smaller SBH of 0.6 eV shows smaller response of 132% for 30 min exposure to 20 ppm NO₂, compared to the diode in Figure 3a with a SBH of 0.65 eV, which exhibits 716% response under similar test conditions. On the other hand, for NH₃ (550 ppm) a larger 90% change at –4 V bias with 10 min exposure in dark is observed for a ~0.59 eV SBH diode, compared to the larger SBH (~0.64 eV) diode in Figure 3b, which shows 13% change under similar test conditions. It should also be noted that variability in the graphene sensors can be caused by environmental issues as well as material imperfections.^[34] Since the performance of the sensor depends on the equilibrium SBH, which can be strongly affected by both these factors, the various steps leading to the sensor realization (i.e., synthesis, transfer and device fabrication) need to be carefully optimized to minimize their impact.

In general, for sensors made of 3D materials, the current transient saturation happens when all possible surface states are occupied by the adsorbing molecules for a given analyte

concentration. Only with 2-dimensional materials like graphene, it is possible for the Fermi level to change due to charge exchange with adsorbed molecules or with application of a reverse bias. If the charge exchange causes the Fermi level to reach the level of the defect energy states induced by the adsorbed molecules then the current transient will saturate even before all possible surface state occupation happens at a given concentration. The effect of reverse bias on the NO₂ and NH₃ sensing transients observed for our sensor clearly indicates that the later mechanism (alignment of graphene Fermi level with defect energy level) is more important in causing current transient saturation in these sensors. This offers interesting possibilities of utilizing the reverse bias as a handle to control the Fermi level and tune the sensitivity as well as the response time of sensors made of appropriate 2D material/semiconductor hetero-junctions.

3. Conclusion

In conclusion, we have demonstrated a reverse-biased graphene/Si heterojunction diode based sensor with ultra-high sensitivity and extremely low operating power, which are orders of magnitude better than conventional chemiresistor type sensors. The ultra-high sensitivity of these sensors

arises out of the exponential dependence of heterojunction reverse current on the SBH, while the reverse bias operation drastically reduces their operating power requirement. The reverse bias operation also enables modulation of the graphene Fermi level, which depends on the magnitude of the reverse bias; enabling both the response time and the sensitivity of the sensors to be tuned as desired. Our results indicate that these 2D material based sensors, unlike their counterparts made of 3D materials, can have their sensing response saturated through alignment of the Fermi level and the adsorbent induced defect states. With careful selection of the 2D material and semiconductor forming the heterojunction, optimized detection of specific analyte is possible, with additional control of the sensor response enabled through appropriate reverse bias and SBH at the heterointerface.

4. Experimental Section

Graphene samples used in this work were synthesized through chemical vapor deposition (CVD) on Cu (catalyst) foils (Alfa Aesar, 99.999% purity) in a quartz tube furnace. The synthesis was performed at 1035 °C and 10 Torr pressure with CH₄ as the precursor (nominal flow rate of 40 sccm) along with H₂ (nominal flow rate 50 sccm), following earlier reports.^[35,36]

To begin with, graphene on copper foil was lithographically patterned and strips were defined by O₂ plasma etch. The Cu foil with graphene strips was coated with two layers of poly methyl methacrylate (PMMA), to add mechanical strength during subsequent processing, and baked for 1 min at 150 °C. Next, the graphene layer on the back side of the sample was removed by oxygen plasma etching, which was followed by Cu etching in 0.5 M ammonium persulfate solution for more than 12 h, releasing the graphene/PMMA bi-layer.^[10] SiO₂ on both p- and n-Si has been selectively removed by 1:5 diluted buffered HF. Ti/Au was deposited on the back side and selectively on top side of Si and annealed in Ar/H₂ atmosphere at 400 °C to make ohmic contacts. After rinsing in deionized water and IPA, the graphene/PMMA bi-layer was scooped and placed on the patterned SiO₂/Si substrate. It was then baked at 220 °C for 5 min to reflow the PMMA resulting in more uniformity and less cracking in transferred graphene. Finally, the sample was placed in acetone for 2 hour to remove PMMA.^[10,37] Ti (20 nm)/Au (80 nm) contacts were evaporated on graphene transferred on SiO₂/Si using shadow mask. The p- and n-Si used in this work are lightly doped and have resistivity in the range of 1–10 Ω cm in both the cases. The graphene/Si interface dimensions vary from 200–1000 μm.

All the electrical and sensing measurements were carried out at room temperature and ambient conditions. The sensor current-voltage characteristics were obtained using a Keithley 2612A System Source Meter. The capacitance-voltage measurements were performed on the sensor using HP 4284A Precision LCR Meter with a frequency range of 20 Hz to 1 MHz. A four terminal pair scheme was used for the measurements. The ac signal amplitude was chosen as 50 mV (rms) with a frequency of 1 kHz. The dc reverse bias was varied from –1 to –4 V.

Supporting Information

Supporting Information is available from the Wiley Online Library or from the author.

Acknowledgements

Financial supports for this work from National Science Foundation (Grant Nos. ECCS-0846898, and ECCS-1029346) is thankfully acknowledged. We would also like to acknowledge Mr. Nicholas DeRoller for his help in generating an illustration.

- [1] A. K. Geim, K. S. Novoselov, *Nat. Mater.* **2007**, *6*, 183.
- [2] K. I. Bolotin, K. J. Sikes, J. Hone, H. L. Stormer, P. Kim, *Phys. Rev. Lett.* **2008**, *101*, 096802.
- [3] F. Schedin, A. K. Geim, S. V. Morozov, E. W. Hill, P. Blake, M. I. Katsnelson, K. S. Novoselov, *Nat. Mater.* **2007**, *6*, 652.
- [4] K. S. Novoselov, A. K. Geim, S. V. Morozov, D. Jiang, M. K. I. Grigorieva, S. V. Dubonos, A. A. Firsov, *Nature* **2005**, *438*, 197.
- [5] K. S. Novoselov, D. Jiang, F. Schedin, T. J. Booth, V. V. Khotkevich, S. V. Morozov, A. K. Geim, *Proc. Natl. Acad. Sci. USA* **2005**, *102*, 10451.
- [6] M. W. Nomani, R. Shishir, M. Qazi, D. Diwan, V. B. Shields, M. G. Spencer, G. S. Tompa, N. M. Sbrockey, G. Koley, *Sens. Actuators, B* **2010**, *150*, 301.
- [7] S. Rumyantsev, L. Guanxiong, R. A. Potyrailo, A. A. Balandin, M. S. Shur, *IEEE Sens. J.* **2013**, *13*, 2818.
- [8] R. A. Potyrailo, C. Surman, N. Nagraj, A. Burns, *Chem. Rev.* **2011**, *111*, 7315.
- [9] S. Rumyantsev, G. Liu, M. S. Shur, R. A. Potyrailo, A. A. Balandin, *Nano Lett.* **2012**, *12*, 2294.
- [10] J. Chan, A. Venugopal, A. Pirkle, S. McDonnell, D. Hinojos, C. W. Magnuson, R. S. Ruoff, L. Colombo, R. M. Wallace, E. M. Vogel, *ACS Nano* **2012**, *6*, 3224.
- [11] A. K. Singh, M. A. Uddin, J. T. Tolson, H. Maire-Afeli, N. Sbrockey, G. S. Tompa, M. G. Spencer, T. Vogt, T. S. Sudarshan, G. Koley, *Appl. Phys. Lett.* **2013**, *102*, 043101.
- [12] C. C. Chen, M. Aykol, C. C. Chang, A. F. J. Levi, S. B. Cronin, *Nano Lett.* **2011**, *11*, 1863.
- [13] X. Li, H. Zhu, K. Wang, A. Cao, J. Wei, C. Li, J. Yi, Z. Li, X. Li, D. Wu, *Adv. Mater.* **2010**, *22*, 2743.
- [14] S. Tongay, T. Schumann, X. Miao, B. R. Appleton, A. F. Hebard, *Carbon* **2011**, *49*, 2033.
- [15] H. Yang, J. Heo, S. Park, H. J. Song, D. H. Seo, K. E. Byun, P. Kim, I. Yoo, H. J. Chung, K. Kim, *Science* **2012**, *336*, 1140.
- [16] H. Y. Kim, K. Lee, N. McEvoy, C. Yim, G. S. Duesberg, *Nano Lett.* **2013**, *13*, 2182.
- [17] A. C. Ferrari, *Solid State Commun.* **2007**, *143*, 47.
- [18] A. C. Ferrari, J. C. Meyer, V. Scardaci, C. Casiraghi, M. Lazzeri, F. Mauri, S. Piscanec, D. Jiang, K. S. Novoselov, A. K. Geim, *Phys. Rev. Lett.* **2006**, *97*, 187401.
- [19] S. M. Sze, *Physics of Semiconductor Devices*, John Wiley, New York, USA **1981**, pp. 245–297.
- [20] R. T. Tung, *Mater. Sci. Eng. R* **2001**, *35*, 1.
- [21] S. Tongay, M. Lemaitre, X. Miao, B. Gila, B. R. Appleton, A. F. Hebard, *Phys. Rev. X* **2012**, *2*, 011002.
- [22] U. Mishra, J. Singh, *Semiconductor Device Physics and Design*, Springer, Dordrecht, The Netherlands, **2007**, 226.
- [23] S. Shivaraman, L. H. Herman, F. Rana, J. Park, M. G. Spencer, *Appl. Phys. Lett.* **2012**, *100*, 183112.

- [24] F. Yavari, E. Castillo, H. Gullapalli, P. M. Ajayan, N. Koratkar, *Appl. Phys. Lett.* **2012**, *100*, 203120.
- [25] Y. Dan, Y. Lu, N. J. Kybert, Z. Luo, A. C. Johnson, *Nano Lett.* **2009**, *9*, 1472.
- [26] J. D. Fowler, M. J. Allen, V. C. Tung, Y. Yang, R. B. Kaner, B. H. Weiller, *ACS Nano* **2009**, *3*, 301.
- [27] R. Pearce, T. Iakimov, M. Andersson, L. Hultman, A. L. Spetz, R. Yakimova, *Sens. Actuators, B* **2011**, *155*, 451.
- [28] G. Chen, T. M. Paronyan, A. R. Harutyunyan, *Appl. Phys. Lett.* **2012**, *101*, 053119.
- [29] M. W. Nomani, V. Shields, G. Tompa, N. Sbrockey, M. G. Spencer, R. A. Webb, G. Koley, *Appl. Phys. Lett.* **2012**, *100*, 092113.
- [30] O. Leenaerts, B. Partoens, F. M. Peeters, *Phys. Rev. B: Condens. Matter Mater. Phys.* **2008**, *77*, 125416.
- [31] R. S. Muller, T. I. Kamins, M. Chan, *Device Electronics for Integrated Circuits*, John Wiley and Sons, New York, USA **2003**, pp. 198-202.
- [32] T. O. Wehling, K. S. Novoselov, S. V. Morozov, E. E. Vdovin, M. I. Katsnelson, A. K. Geim, A. I. Lichtenstein, *Nano Lett.* **2008**, *8*, 173.
- [33] A. A. Balandin, *Nat. Nanotechnol.* **2013**, *8*, 549.
- [34] G. Xu, Y. Zhang, X. Duan, A. A. Balandin, K. L. Wang, *Proc. IEEE* **2013**, *101*, 1670.
- [35] X. Li, W. Cai, J. An, S. Kim, J. Nah, D. Yang, R. Piner, A. Velamakanni, I. Jung, E. Tutuc, *Science* **2009**, *324*, 1312.
- [36] S. Bhaviripudi, X. Jia, M. S. Dresselhaus, J. Kong, *Nano Lett.* **2010**, *10*, 4128.
- [37] J. W. Suk, A. Kitt, C. W. Magnuson, Y. F. Hao, S. Ahmed, J. H. An, A. K. Swan, B. B. Goldberg, R. S. Ruoff, *ACS Nano* **2011**, *5*, 6916.

Received: August 28, 2013
Revised: November 6, 2013
Published online: December 23, 2013